Available online at www.sciencedirect.com

SCIENCE DIRECT®

Experimental Cell Research 300 (2004) 320–334

Experimental Cell Research

www.elsevier.com/locate/yexcr

Replication protein A and γ-H2AX foci assembly is triggered by cellular response to DNA double-strand breaks

Adayabalam S. Balajee*, Charles R. Geard

Center for Radiological Research, Department of Radiation Oncology, College of Physicians and Surgeons, Columbia University, New York, NY 10032, United States

Received 12 January 2004, revised version received 6 July 2004
Available online 27 August 2004

Abstract

Human replication protein A (RPA p34), a crucial component of diverse DNA excision repair pathways, is implicated in DNA double-strand break (DSB) repair. To evaluate its role in DSB repair, the intranuclear dynamics of RPA was investigated after DNA damage and replication blockage in human cells. Using two different agents [ionizing radiation (IR) and hydroxyurea (HU)] to generate DSBs, we found that RPA relocated into distinct nuclear foci and colocalized with a well-known DSB binding factor, γ-H2AX, at the sites of DNA damage in a time-dependent manner. Colocalization of RPA and γ-H2AX foci peaked at 2 h after IR treatment and subsequently declined with increasing postrecovery times. The time course of RPA and γ-H2AX foci association correlated well with the DSB repair activity detected by a neutral comet assay. A phosphatidylinositol-3 (PI-3) kinase inhibitor, wortmannin, completely abolished both RPA and γ-H2AX foci formation triggered by IR. Additionally, radiosensitive ataxia telangiectasia (AT) cells harboring mutations in ATM gene product were found to be deficient in RPA and γ-H2AX colocalization after IR. Transfection of AT cells with ATM cDNA fully restored the association of RPA foci with γ-H2AX illustrating the requirement of ATM gene product for this process. The exact coincidence of RPA and γ-H2AX in response to HU specifically in S-phase cells supports their role in DNA replication checkpoint control. Depletion of RPA by small interfering RNA (SiRNA) substantially elevated the frequencies of IR-induced micronuclei (MN) and apoptosis in human cells suggestive of a role for RPA in DSB repair. We propose that RPA in association with γ-H2AX contributes to both DNA damage checkpoint control and repair in response to strand breaks and stalled replication forks in human cells.

Keywords: Double-strand break repair; Replication protein A; Histone H2AX; Ataxia telangiectasia; Replication blockage

Introduction

Replication protein A (RPA) plays important roles in diverse DNA metabolic activities such as replication, repair, and recombination [1]. RPA occurs in a heterotrimeric form comprising three subunits with a molecular mass of 70 kDa (p70), 34 kDa (p34), and 14 kDa (p14), respectively. RPA facilitates the DNA unwinding process during replication initiation and elongation and participates in the DNA damage recognition step of nucleotide excision repair pathway [2–4] through its interaction with XPA (xeroderma pigmentosum complementation group A) and XPG (XP group G) proteins. RPA also enhances the endonuclease activities of XPF-ERCC1 and XPG [5]. RPA is additionally involved in the long patch base excision repair pathway that removes the oxidized base lesions from the genomic DNA [6]. Evidence for the stimulation of DNA ligase I activity by RPA has been recently obtained [7]. RPA catalyzes the homologous pairing and DNA strand exchange steps through its interaction with recombination proteins Rad51 and Rad52 [8].

Among the three subunits, RPA (p34) is a phosphoprotein, which is differentially phosphorylated during the

Abbreviations: ATM, ataxia telangiectasia mutated; RPA, replication protein A; DSB, double strand break; γ-H2AX, phosphorylated histone H2AX; PI-3, phosphatidylinositol-3 kinase; HU, hydroxyurea.

* Corresponding author. Center for Radiological Research, Department of Radiation Oncology, College of Physicians and Surgeons, Columbia University, VC-11, Room 243, 168th Street, 630 West, New York, NY 10032. Fax: +1 212 305 3229.
E-mail address: ab836@columbia.edu (A.S. Balajee).

0014-4827/$ - see front matter © 2004 Elsevier Inc. All rights reserved.
doi:10.1016/j.yexcr.2004.07.022

progression of cells from G1 to S-phase, and becomes hyperphosphorylated in response to DNA damage induced by ionizing radiation (IR), ultraviolet radiation (UV), and DNA replication inhibitors such as hydroxyurea (HU) and aphidicolin (APC). RPA phosphorylation by DNA damage is either attenuated or abolished in cells defective in DNA-dependent protein kinase (DNA-PK) and ataxia telangiectasia mutated (ATM) genes [9,10], indicating their involvement in RPA (p34) phosphorylation. A direct role for DNA-PK in RPA phosphorylation in response to replication mediated DNA damage by topoisomerase I inhibitor, camptothecin, has been demonstrated [9]. ATM kinase is a crucial factor for initiating a cascade of signal transduction pathways in response to IR treatment. Many well-known double-strand break (DSB) repair factors such as Nbs1, Mre11, and BRCA1 are phosphorylated in response to IR by ATM kinase [11–13]. Colocalization of RPA and ATM kinase has been reported in the synaptonemal complex of meiotic chromosomes suggestive of functional interaction during homologous recombination [14]. The involvement of RPA both in nonhomologous end-joining (NHEJ) and homologous recombination repair (HRR) pathways has also emerged recently. Perrault et al. [15] demonstrated that DSB rejoining by the NHEJ pathway is facilitated by RPA in vitro, while the nuclear foci formation of RPA after IR is modulated by the functional status of BRCA1 [16]. Interaction of RPA with BRCA1, Rad51, and Rad52 proteins attests to a role for RPA in the recombinational repair of DSBs. MacPhail and Olive [17] suggested that the persistence of RPA foci several hours after IR represents sites of irreparable lesions, and this phenomenon might facilitate identification of radiosensitive cells. Nevertheless, the precise participation of RPA in DSB repair is far from clear.

Investigation of the intranuclear dynamics of RPA foci formation in relation to well-known DSB repair factors may enhance our understanding of RPA participation in DSB repair. With this objective in mind, we have undertaken a microscopy-based approach to characterize the RPA foci formation in response to DNA strand breaks generated by IR and HU. To determine whether the focal sites of RPA form at DSB sites, RPA foci formation was analyzed in combination with a well-known DSB binding factor, phosphorylated histone H2AX (γ-H2AX). Using two different agents to generate DSBs, we found that RPA foci colocalized with γ-H2AX in a time-dependent manner after DNA damage. The time course of RPA and γ-H2AX foci association exactly coincided with the DSB repair kinetics detected by a modified neutral comet assay. Absence of RPA and γ-H2AX foci association after IR in radiation-sensitive AT cells suggests a role for ATM gene product in mediating this response. Our findings suggest that DNA damage-dependent recruitment of RPA to γ-H2AX containing focal sites may comprise a critical DNA damage checkpoint control and repair component in human cells.

Materials and methods

Cell lines and culture conditions

Human fibroblast cell lines established from normal (MRC5 and GM637H) and AT (GM8391A and GM5849C) individuals were obtained from Coriell Cell Repository, Camden, NJ. Cells were routinely maintained in 2× Eagle minimal essential medium (E-MEM) supplemented with 15% fetal bovine serum, vitamins, essential amino acids, nonessential amino acids, and antibiotics (Gibco BRL). The cultures were maintained at 37°C in a humidified 5% CO_2 atmosphere.

Generation of ATM cDNA-transfected cell lines

Dr. Yosef Shiloh (University of Tel Aviv, Israel) generously provided the plasmid DNA-harboring empty vector (pEBS7) and ATM cDNA (pEBS7-YZ5). Procedures for the construction of these plasmids as well as the complementation of AT cells by ATM cDNA have been previously described [18]. SV-40-transformed AT fibroblast cells (GM5849C) in exponential growth phase were transfected with 10 μg of DNA. Transfected cells were grown in the presence of hygromycin (200 μg/ml), and the stable cell lines were generated from hygromycin-resistant colonies.

Treatment of cells with γ-irradiation and replication inhibitors

Cells in exponential growth phase were irradiated with γ-rays (0, 1, 10, or 20 Gy) using a ^{137}Cs source at a dose rate of 0.98 Gy/min (Gamma cell 40, Atomic Energy of Canada, Canada). To inhibit phosphatidylinositol-3 (PI-3)-like kinases, wortmannin (20 μM) was added to the cells 1 h before IR, and the cells were postincubated for 2 h after IR in the presence of wortmannin. For replication blockage, cells in exponential growth phase were treated with 5 mM HU (Sigma) for 3 h.

Colocalization of γ-H2AX and RPA sites in interphase nuclei

Cells were grown on glass chamber slides for immunofluorescence (Labtek). After different recovery times, cells were fixed for 10 min in ice-cold acetone–methanol (1:1). The slides were washed in TBST (20 mM Tris-HCl pH 7.4, 137 mM NaCl, and 0.2% Tween 20) and incubated for 30 min in TBST containing 5% nonfat dried milk (NFDM). The slides were again washed in TBST and incubated with the primary antibodies for γ-H2AX (1:50 dilution in TBST–5% NFDM; rabbit polyclonal, Upstate Biotechnology, New York) and p34 subunit of RPA (1:25 dilution in TBST–5% NFDM; mouse monoclonal, Neomarkers) for 1 h at 37°C. The slides were then washed three times for 5 min each in TBST buffer and incubated for 1 h at 37°C with FITC-

conjugated antirabbit IgG and Texas red-conjugated anti-mouse IgG (1:50 dilution in TBST–5% NFDM; Vector laboratories). A final wash in TBST was followed by counterstaining DNA with DAPI (0.1 μg/ml prepared in Vectashield mounting medium; Vector laboratories). The images were captured using both Axioplan2 Imaging microscope (Zeiss) and a laser confocal microscope (Nikon).

Neutral comet assay

The neutral comet assay for the detection of DSB was carried out essentially as described by Wojewodzka et al. [19]. One major modification introduced in this assay was the lysis of cells at 4°C instead of 50°C which would prevent the conversion of IR-induced heat-labile sites into DSBs. Briefly, comet slides (Trevigen) were prepared by mixing 10 μl of cell suspension (5×10^5 cells/ml) with 90 μl of low-melt agarose (Sigma Type VII) at a final concentration of 0.75%. After solidification, slides were lysed at 4°C for 1 h in a buffer (2.5 M NaCl, 100 mM EDTA, 10 mM Tris-HCl, 1% N-lauroylsarcosine, 0.5% Triton X-100, and 10% dimethylsulfoxide, pH 9.5). The slides were washed three times in electrophoresis buffer (300 mM sodium acetate and 100 mM Tris-HCl, pH 8.3) and left in the buffer for 1 h. The slides were electrophoresed for 1 h at 20 V at 8°C. Comet images stained with Cyber Green (1 μg/ml) were captured using a laser confocal microscope (Nikon). The tail moment was analyzed using Euclid comet analysis software.

Protein extraction, SDS-PAGE, and Western blot analysis

Soluble and insoluble proteins were isolated essentially as described [20]. At different postincubation times, $6–8 \times 10^6$ treated and mock-treated cells were lysed for 8 min on ice in 500 μl of hypotonic buffer (10 mM Tris-HCl pH 7.4, 2.5 mM $MgCl_2$, 1 mM PMSF, and 0.5% Nonidet P-40). The cell lysates were centrifuged at 3000 rpm for 5 min, and the soluble proteins (supernatant) were transferred to a fresh tube. The pellet fraction containing the detergent-resistant proteins was lysed for 20 min with 200 μl of 20 mM sodium phosphate buffer (pH 8.0) containing 0.5 M NaCl, 1 mM EDTA, 0.75% Triton X-100, 10% glycerol, 5 mM $MgCl_2$, 1 mM PMSF. To release the chromatin-associated proteins, the cell extract was incubated for 15 min on ice with 50 units of RNase-free DNase I. The proteins were recovered by centrifugation at 12,000 rpm for 5 min. Protein concentration was determined with the Pierce protein assay kit. Soluble and insoluble proteins (25 μg) were fractionated by 4–20% polyacrylamide gradient gel electrophoresis and blotted onto PVDF membrane following the standard protocol (Novex). The immunological detection of RPA and γ-H2AX was performed using a standard protocol (Enhanced chemiluminescence procedure of Amersham). The membranes were also reacted with actin antibody (goat IgG, 1:1000 dilution, Santa Cruz Biotechnology) to verify the equal loading of proteins. The band intensity relative to actin protein was measured using Kodak 1D image analysis software (Kodak).

Small interfering RNA (SiRNA) transfection

SiRNA transfection was performed using siPORT Amine following the guidelines of Ambion. Exponentially growing cells (70% confluence) in 60-mm dishes were incubated with transfection reagent (6 μl of transfection reagent diluted to 197 μl in OPTI-MEM, Invitrogen) and 75 nM of either control SiRNA [glyceraldehyde 3-phosphate dehydrogenase (GAPDH), Ambion] or RPA (p34 subunit) SiRNA (5′-GGCUCCAACCAACAUUGUUdTdT-3′, annealed, and HPLC- and PAGE-purified, Ambion) for 8 h. Cells were analyzed 72 h after SiRNA transfection. RPA expression was analyzed by immunofluorescence and Western blot techniques. The transfection efficiency of the cells was separately determined by the use of GFP-pc 3.1 plasmid.

Analyses of micronuclei (MN) and apoptosis

Two commonly used biological endpoints, MN and apoptosis, were chosen to evaluate the role of RPA in DSB repair. MN formation is considered to be a reliable indicator for chromosome breakage and loss resulting from either misrepair or lack of DSB repair. Non-transfected and SiRNA-transfected GM637H cells (72 h after transfection) cultured in 2-well chamber slides (Labtek) were irradiated with 10 Gy of γ-rays and postincubated for 24 h at 37°C in complete medium. Cells after fixation in acetone–methanol were immunostained for γ-H2AX and RPA followed by counterstaining with DAPI. At least 500 randomly chosen mononucleated cells were scored for MN for each treatment, and the frequency of MN was expressed as MN/cell. To verify the analysis of MN by DAPI, cells were also separately stained with acridine orange (3 μg/ml in PBS) which exhibits a differential staining of cytoplasm (red) and nucleus (green). Images were captured using a laser confocal microscope (Nikon).

Apoptosis was detected by two independent approaches: in the first approach, apoptotic cells were identified by DNA fragmentation and intense γ-H2AX staining. In the second approach, apoptotic cells were detected by a TUNEL (terminal deoxynucleotidyl transferase dUTP Nick End labeling) assay (apo-BrdU-TUNEL assay kit, Molecular Probes) following the manufacturer's specifications. For TUNEL assay, control and irradiated cells after 24 h were trypsinized and fixed in 1% paraformaldehyde followed by a second fixation in 70% ethanol. After washing in PBS, cell pellets were treated with 50 μl of reaction mixture containing terminal deoxynucleotidyl transferase and bromodeoxyuridine triphosphate (BrdUTP) for 1 h at 37°C. Apoptotic

cells were detected by Alexa Fluor 488-conjugated anti-BrdU antibody. The cells were counterstained with propidium iodide (PI, 0.1μg/ml). The cells were microscopically examined, and the images were captured using a confocal laser-scanning microscope (Nikon).

DNA end-joining reaction

Plasmid pBluescript II (Ks+) was obtained from Stratagene. Supercoiled plasmid DNA linearized with either *Eco*RI or *Bam*HI was used as a substrate for the end-joining reaction. End-joining reactions were carried out for 1 h at 37°C in a buffer (20 mM HEPES-KOH pH 7.5, 10 mM $MgCl_2$, 80 mM KCl, 1 mM ATP, and 1 mM DTT) containing 0.5 μg of plasmid DNA and the whole cell extracts (WCE) prepared from SV-40-transformed normal human fibroblast (GM637H) cells. End-joining reactions carried out in the absence of extracts served as a negative control. The reactions were terminated by the addition of SDS (1%) and proteinase K (50 μg/ml), and the samples were incubated at 37°C for 1 h. The samples were loaded on a 0.75% agarose gel. End-joining products were quantified by Kodak 1D image analysis software.

Results

DNA damage-dependent colocalization of RPA and γ-H2AX foci

The time course of intranuclear distribution of RPA in relation to γ-H2AX foci was examined in SV-40-transformed normal human fibroblasts (GM637H) after IR (1 or 10 Gy of γ-rays irradiation) in comparison to unirradiated cells using a combination of antibodies specific for RPA and γ-H2AX. Two distinct patterns of RPA were observed in the nuclei of unirradiated cells directly fixed in acetone–methanol (1:1). A homogenous distribution of small RPA foci ranging from 300 to 350 in number was observed in a great majority of cells (approximately 88%), while the remainder of the cells displayed 8–10 large RPA focal sites. Similarly, two patterns of γ-H2AX foci were found in unirradiated cells. γ-H2AX staining was weak and diffuse in more than 85% of the cells. In the remainder of the cells, 10–12 bright γ-H2AX foci were noticed, out of which a few (4–6) exactly coincided with that of RPA foci. These sites probably represent the spontaneous occurrence of DSBs in the absence of exogenous damage. The homogenous RPA distribution observed in unirradiated control cells relocated into distinct nuclear foci after irradiation (Fig. 1A). Upon irradiation with γ-rays, several hundreds of phosphorylated H2AX (γ-H2AX) foci were detected in GM637H cells. γ-H2AX foci rapidly appeared during and after irradiation (10 min irradiation time; no recovery), and the fluorescence intensity peaked at 30 min after irradiation (Fig. 1) with a subsequent decline with increasing post-irradiation times. Coincidence of RPA and γ-H2AX foci was detectable at 30 min after IR, but the exact coincidence detected at 2 h after γ-rays indicated a time-dependent association of both proteins at the DSB sites (Fig. 1A). An enlarged portion of an interphase nucleus showing the exact coincidence of both RPA and γ-H2AX is given in Fig. 1B. A quantitative assessment of RPA and γ-H2AX colocalization by counting all of the foci in at least 30 randomly chosen cells per time point is shown in Fig. 1C. Colocalization of RPA and γ-H2AX persisted through 8 h after IR, although the number of foci showing colocalization decreased dramatically in each and every cell at the later time points (Fig. 1C). γ-H2AX is considered to be tightly associated with chromatin. Attempts to immunoprecipitate RPA and γ-H2AX complex using either of the antibodies were not successful. Only a small fraction of γ-H2AX gets solubilized in low salt buffer, and solubilization of histones requires extraction with 100 mM HCl that might disrupt the protein–protein interactions. Thus far, studies showing colocalization of γ-H2AX with other known DSB repair factors such as BRCA1, Rad51, and Rad52 have all been done by immunofluorescence probably due to this technical problem. Alternatively, these two proteins may interact with each other either through DNA or some other protein factor.

Colocalization of RPA and γ-H2AX after a low dose of irradiation

To evaluate the functional significance of RPA and γ-H2AX foci formation under physiologically relevant doses, immunofluorescence analysis was carried out in both SV40-transformed (GM637H) and primary (MRC5) normal human fibroblast cells after 1 Gy of γ-rays. The choice of 1 Gy is considered to be physiologically relevant as survival experiments revealed more than 85% cloning efficiency of GM637H cells after 1 Gy of γ-rays (data not shown). IR-induced RPA and γ-H2AX foci were easily detectable in both cell lines after 1 Gy of IR. In GM637H cells irradiated with 1 Gy of γ-rays, efficient γ-H2AX and RPA colocalization was observed at 1h in 70% of the cells illustrating the high sensitivity of this complex formation in response to DNA strand breaks induced by a low dose of IR (Fig. 1D). Similarly, efficient colocalization of RPA with γ-H2AX was observed after 1 h in MRC5 cells (Fig. 1E). However, RPA and γ-H2AX foci association was almost completely diminished by 3 h after 1 Gy of IR, unlike 10 Gy of γ-rays, and at 8 h, γ-H2AX foci were hardly detectable. This indicates that the kinetics of RPA and γ-H2AX foci assembly and their dissociation are dependent on the extent of initial DNA damage. A quantitative assessment made on RPA and γ-H2AX colocalization by counting all of the foci in at least 50 randomly chosen unirradiated and irradiated cells is given in Fig. 1E. The analysis revealed that 65.84% of RPA foci completely coincided with that of γ-H2AX after 1 Gy of IR in MRC5 cells.

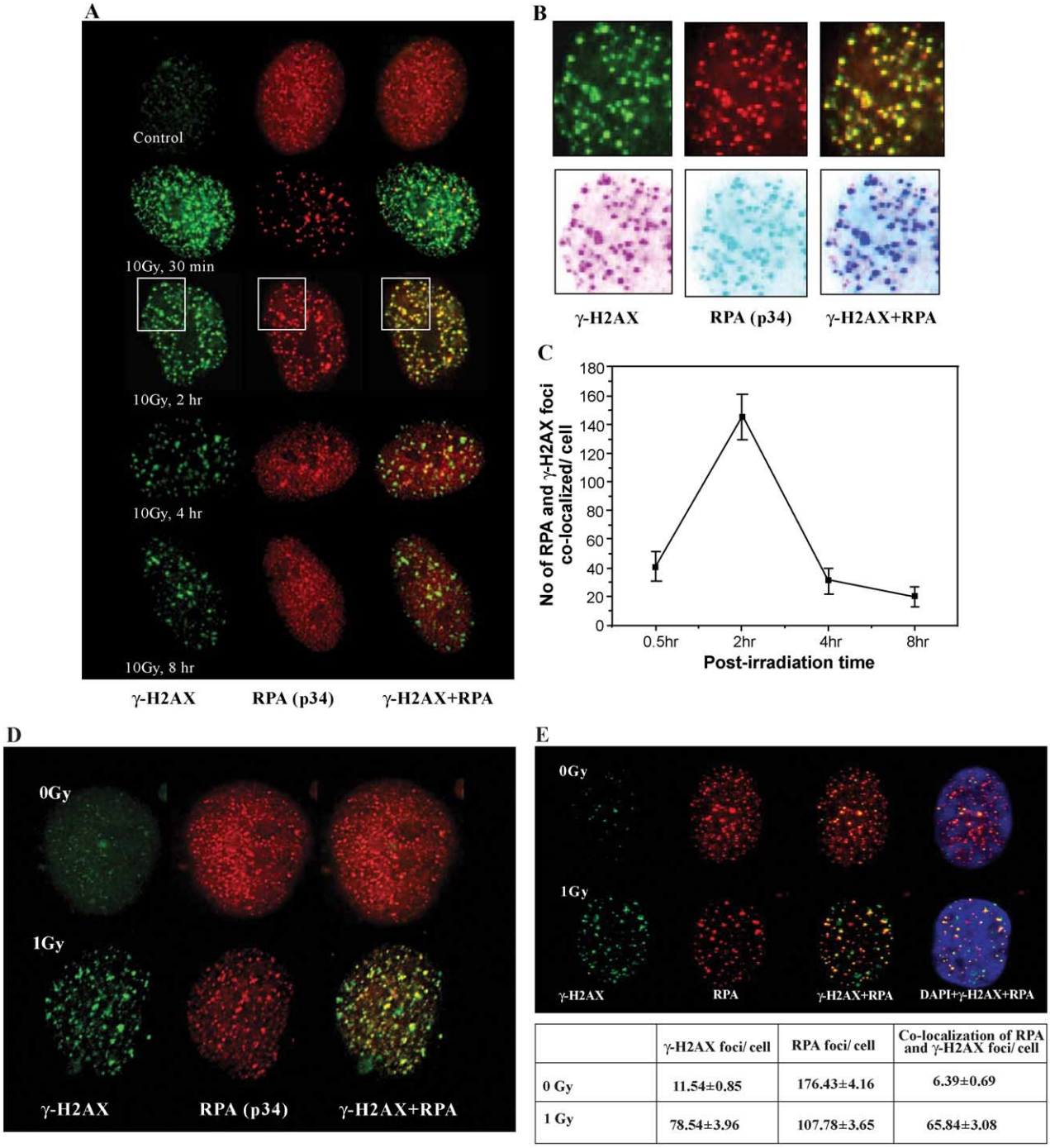

	γ-H2AX foci/ cell	RPA foci/ cell	Co-localization of RPA and γ-H2AX foci/ cell
0 Gy	11.54±0.85	176.43±4.16	6.39±0.69
1 Gy	78.54±3.96	107.78±3.65	65.84±3.08

Fig. 1. Ionizing radiation triggers the colocalization of RPA and γ-H2AX in a time dependent-manner in human cells. (A) Asynchronously growing SV-40-transformed GM637H cells were irradiated with 10 Gy of γ-rays and incubated at 37°C for different recovery times. The cells were fixed in acetone-methanol and immunostained for RPA and γ-H2AX. IR triggered the induction of γ-H2AX and RPA focal distribution, and the sequestration of both proteins at DSB sites peaked at 2 h. Cells shown in A are representative of more than 85% of the total population observed at different time points after IR. (B) A portion of the interphase nucleus is enlarged in the top panel to illustrate the coincidence of γ-H2AX and RPA at 2 h after IR. The inverted images of RPA and γ-H2AX in the bottom panel show the merging of two colors. A quantitative assessment made on the number of RPA and γ-H2AX foci colocalized cell by microscopic analysis of at least 30 cells for each time point is illustrated in C. Error bars represent the standard error of the mean. Colocalization of RPA and γ-H2AX induced by 1 Gy of γ-rays in human fibroblast cells [GM637H (D) and MRC5 (E)]. Cells in exponential growth phase were irradiated, and the cells were incubated at 37°C for 1 h. The cells were fixed in acetone-methanol and immunostained for RPA and γ-H2AX. A quantitative assessment was made by counting all of the foci in 50 randomly chosen MRC5 cells to determine the extent of colocalization between RPA and γ-H2AX (E). Values represent the mean number of foci/cell and the standard error of the mean.

Time course formation of γ-H2AX and RPA assembly correlates with DSB repair kinetics

To determine whether the time course of RPA and γ-H2AX foci formation reflects DSB repair kinetics, a modified neutral comet assay was performed to assess repair rates. The modification involved the lysis of cells at 4°C instead of 50°C. This is particularly important as some of heat-labile sites generated by IR can be converted into DSBs. Analysis of tail moment in 75 comets for each time point revealed that 28% of the DSBs were repaired at 30 min after IR, while 62% and 82% of the DSBs were repaired by 2 and 4 h after IR, respectively (Fig. 2). Representative images of neutral comets along with the tail moments observed at different recovery times after IR are shown in Fig. 2. In correlation with DSB repair activity, the number of foci with RPA and γ-H2AX colocalization showed a rapid increase during the initial 2 h after IR during which 62% of the DSBs generated by IR were repaired. The percentage of cells showing RPA- and γ-H2AX-colocalizing foci (Fig. 2) as well as their number on a cell-to-cell basis subsequently declined with increasing post-irradiation times (Fig. 1C). Colocalization of γ-H2AX and RPA, which was observed in more than 80% of the cells at 2 h, was gradually diminished at 4 h (59%) and 8 h (22%) after irradiation.

AT cells are defective in RPA and γ-H2AX colocalization

To validate the functional relevance of this complex in IR-induced DNA strand breaks, we investigated the efficiency of RPA and γ-H2AX focus formation in AT cells defective in PI-3-related ATM kinase. For this purpose, we generated two isogenic cell lines for comparison by transfecting AT cells (GM5849C) with plasmid containing either empty vector (pEBS7) or FLAG epitope-tagged ATM cDNA (pEBS7-YZ5). Cytotoxicity assays revealed that transfection of ATM cDNA conferred resistance to AT cells upon exposure to IR and hydrogen peroxide treatment (data not shown). Stably transfected cell lines generated on the basis of hygromycin resistance were irradiated with 10 Gy and immunologically analyzed for γ-H2AX and RPA assembly. In contrast to normal human cells, AT cells transfected with vector alone failed to show the focal redistribution of RPA in response to IR. Furthermore, the induction of γ-H2AX foci formation was also greatly attenuated (Fig. 3). The low level of γ-H2AX foci induction observed in AT cells after IR may be due to PI-3-like kinases other than ATM. The homogenous RPA distribution remained unaltered both in un-irradiated and irradiated AT cells transfected with vector alone. The percentage of cells showing colocalization of RPA and γ-H2AX after 30 min

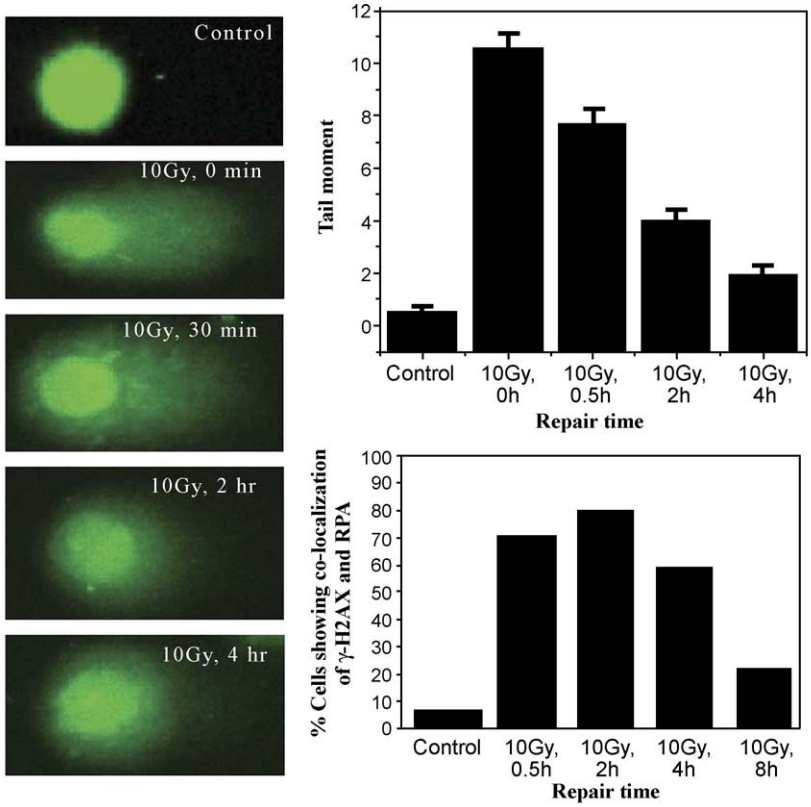

Fig. 2. Analysis of time course kinetics of DSB repair by a neutral comet assay. GM637H cells were irradiated with 10 Gy of γ-rays and postincubated for various recovery times. For the determination of initial induction of DNA damage (0 min after IR), cells were irradiated on ice. Comet slides were prepared, lysed in a neutral buffer, and electrophoresed. Comet images were captured using a laser confocal microscope (Nikon), and the tail moment was analyzed in 70–75 randomly chosen comets using Euclid Comet analysis software. Representative comet images and the tail moment as well as percentage of cells showing colocalization of RPA and γ-H2AX observed at different times are shown. Error bars represent the standard error of the mean.

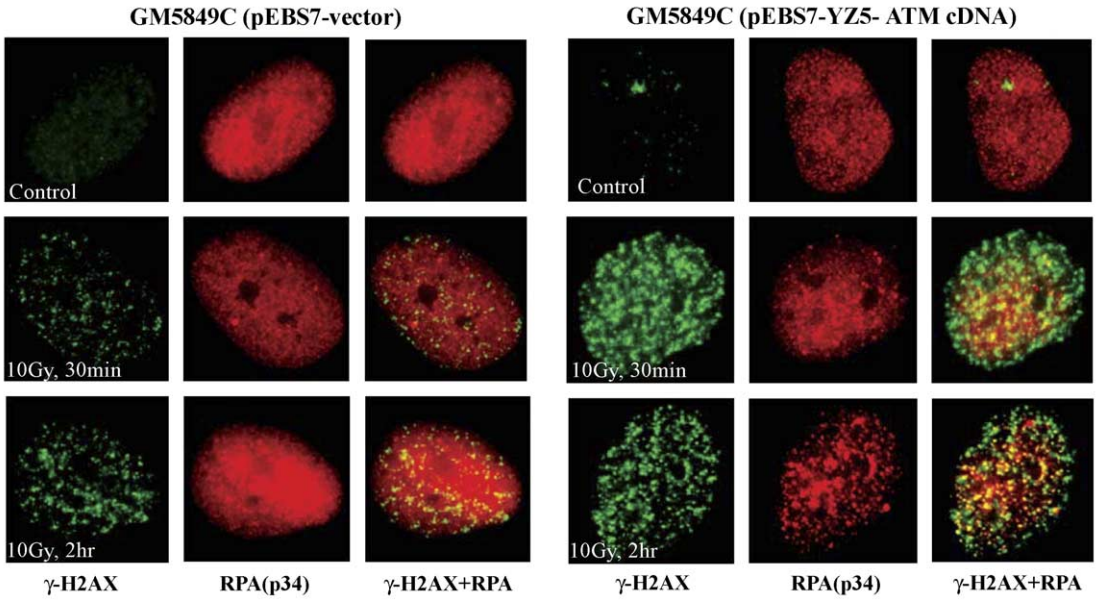

	% cells showing co-localization of RPA and γ-H2AX	
	GM5849C (pEBS7-vector)	GM5849C (pEBS7-YZ5- ATM cDNA)
Control	8	14
10Gy, 30 min	17	62
10Gy, 2hr	14	76

Fig. 3. ATM gene product is critical for RPA and γ-H2AX foci formation. GM5849C cells were transfected either with vector (pEBS7) or ATM cDNA (pEBS7-YZ5). Stably transfected cells were irradiated with 10 Gy of γ-rays and fixed at different recovery times. Cells were immunostained for RPA and γ-H2AX. Transfection of ATM cDNA fully restored the colocalization of RPA and γ-H2AX in AT cells. Images were captured using a laser confocal microscope (Nikon), and the incidence of colocalization was analyzed in 100 randomly chosen cells for each cell line. The percentage of cells showing the colocalization of RPA and γ-H2AX in both cell lines is given in a tabular form.

and 2 h after IR was low (27% and 18% of that in proficient cells, Fig. 3) in AT cells after IR, and within this population, very few RPA foci [12–18] showed colocalization with γ-H2AX. In contrast, the percentage of cells showing RPA and γ-H2AX colocalization greatly increased after IR in AT cells transfected with ATM cDNA (Fig. 3), and more than 70% of RPA foci were found to coincide with that of γ-H2AX when a quantitative analysis was done on a cell-to-cell basis. These findings clearly demonstrate a critical role for ATM in mediating RPA and γ-H2AX foci association in response to IR.

RPA and γ-H2AX foci colocalize in response to replication blockage in human cells

If γ-H2AX and RPA assembly is specific for DSBs, agents other than IR that induce DSBs should also trigger this complex formation. To examine this possibility, the specificity of RPA and γ-H2AX foci association was examined in human cells after treatment with HU that induces DSBs at the sites of stalled replication forks. In untreated control cells, the pattern of RPA and γ-H2AX foci was essentially similar as described before (Fig. 4A). In control cells, RPA foci distribution was more homogenous throughout the nucleoplasm. To enhance the resolution and the accuracy of RPA foci counting, four to five optical sections of the interphase nuclei were taken using laser confocal microscope, and the median section was used for foci counting. Upon HU treatment, numerous small RPA foci were transformed into large focal sites, and 88% of the total RPA foci coincided with γ-H2AX (Figs. 4A and B). The percentage of cells showing colocalization of γ-H2AX and RPA corresponded well with the percentage of cells in S-phase detected with a PCNA antibody (data not shown). Colocalization of RPA and γ-H2AX foci was found to persist in cells 3 h after the removal of HU at which time numerous small RPA and γ-H2AX foci were noticed. Quantitative assessment made on at least 30 randomly chosen cells revealed that 53% of RPA foci coincided with γ-H2AX in cells at 3 h after the removal of HU (Fig. 4B). The observation of RPA and γ-H2AX colocalization specifically in S-phase cells indicates the specificity as well as the functionality of their association in response to DSBs. To verify whether RPA colocalizes with any other known DNA repair/replication proteins, its association with PCNA (a processivity factor

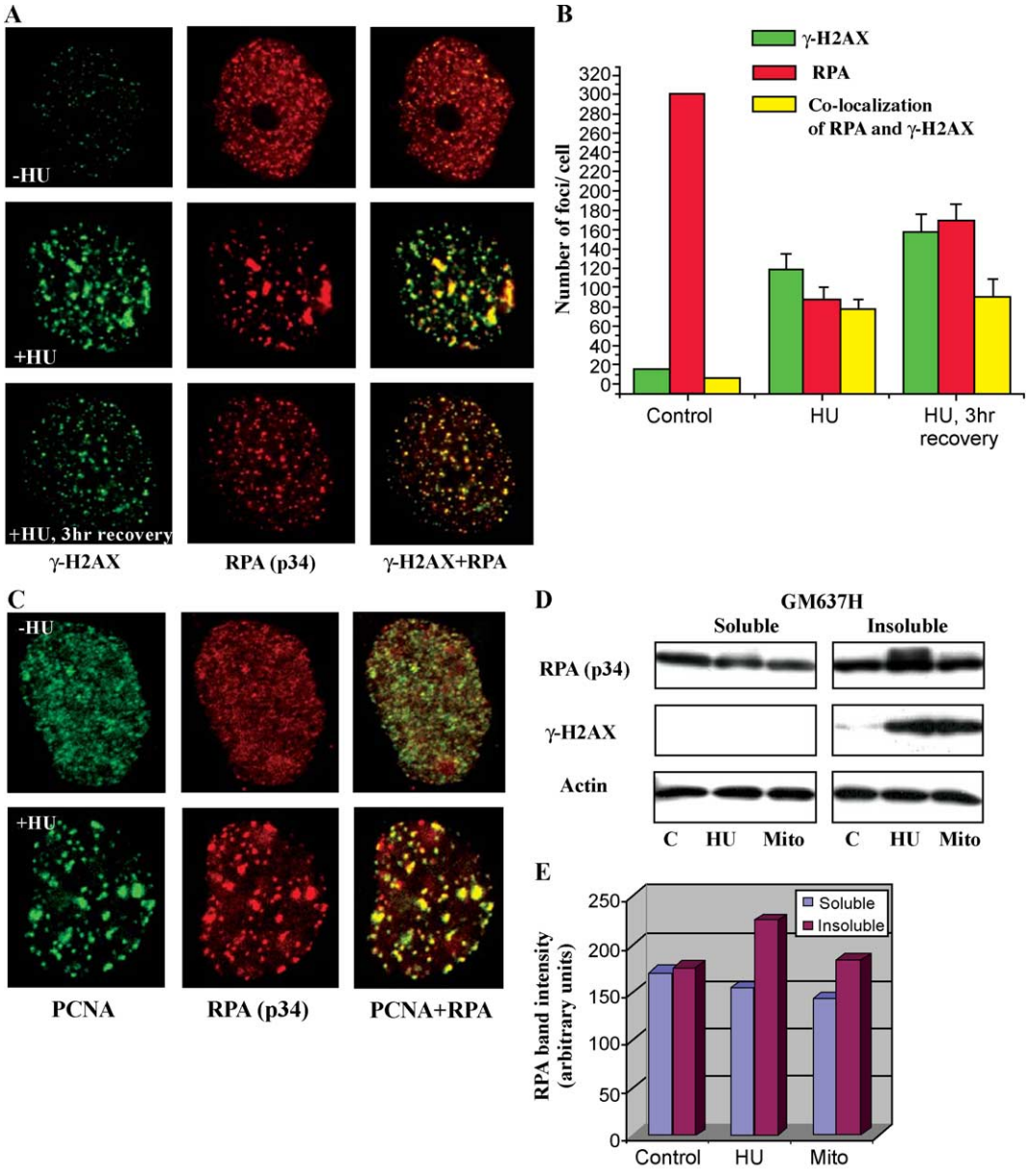

Fig. 4. Replication blockage induces the assembly of RPA and γ-H2AX in normal human cells. GM637H cells in exponential growth phase were treated with HU (5 mM) for 3 h. The cells were either directly fixed in acetone–methanol or allowed to grow in the complete medium for 3 h in the absence of HU. The cells were immunostained for γ-H2AX and RPA to determine the coincidence of both proteins at the stalled replication forks (A). The number of RPA foci colocalized with γ-H2AX was determined on a cell-to-cell basis by the quantitative analysis of at least 30 randomly chosen cells. Error bars indicate the standard error of the mean (B). (C) Colocalization of RPA with PCNA in response to replication blockage in human cells. GM637H cells in exponential growth phase were treated with HU (5 mM) for 3 h and were directly fixed in acetone–methanol. The cells were immunostained for RPA and PCNA to determine the coincidence of both proteins at the sites of stalled replication forks. (D) Exponentially growing GM637H cells were treated with HU (5 mM) and mitoxantrone (50 ng/ml) for 3 h. Soluble and insoluble proteins were isolated (see Materials and methods), and 25 μg of proteins from both fractions was resolved on a 4–20% SDS–polyacrylamide gel electrophoresis. The proteins were transferred to PVDF membrane and immunoreacted with antibodies for RPA, γ-H2AX and actin. The intensity of RPA band in different lanes was quantitated using Kodak 1D image analysis software (E) relative to the level of actin, which was used as a loading control.

for DNA polymerase δ and ε) was analyzed after HU. Analogous to RPA and γ-H2AX, RPA foci exactly coincided with that of PCNA at the sites of stalled replication forks (Fig. 4C) in S-phase cells. These observations suggest that RPA-associated protein complex accumulates at the sites of DNA strand breaks generated by replication blockage.

Chromatin association of RPA is enhanced by replication blockage

We have observed that the colocalization of RPA and γ-H2AX triggered by HU persisted in cells even after the removal of soluble proteins by extraction with a hypotonic buffer containing 0.5% NP40 detergent. This raises the

possibility that colocalization of RPA with γ-H2AX observed specifically in S-phase after HU treatment may be partially mediated by the enhanced association of RPA with chromatin at the stalled replication forks. To determine if RPA is specifically enhanced in chromatin-associated protein fraction, RPA distribution was analyzed in soluble and insoluble (chromatin bound) proteins isolated from cells treated with HU and mitoxantrone (a topoisomerase II inhibitor which induces replication-mediated DSBs at the stalled replication forks). In control cells, 45% of total RPA was found in the insoluble fraction. In HU- and mitoxantrone-treated cells, the chromatin-bound RPA was enhanced to 59% and 53%, respectively (Figs. 4D and E). Furthermore, RPA phosphorylation (judged by the slower migrating band of RPA) triggered by HU was specifically enriched in chromatin-bound protein fraction. As expected, HU and mitoxantrone rapidly induced γ-H2AX only in the chromatin-bound insoluble fraction. Specific enrichment of both RPA and γ-H2AX proteins in the chromatin-associated fraction of S-phase cells suggests that both proteins participate in DNA damage/replication checkpoint control machinery.

RPA silencing does not affect γ-H2AX foci formation after IR

To evaluate the role of RPA in DSB repair, IR-induced DNA damage response was analyzed in cells in which SiRNA suppressed RPA expression. Western blot analysis revealed that RPA level was unaltered in cells transfected with a control GAPDH SiRNA, while RPAp34-specific SiRNA used in the present study was very effective in suppressing RPA expression (Fig. 5A). Immunofluorescence analysis using RPA antibody indicated that more than 85% of the RPA SiRNA-transfected cells were negative for RPA staining (Fig. 5B). GAPDH SiRNA- and RPA SiRNA-transfected cells were next examined for their ability to form

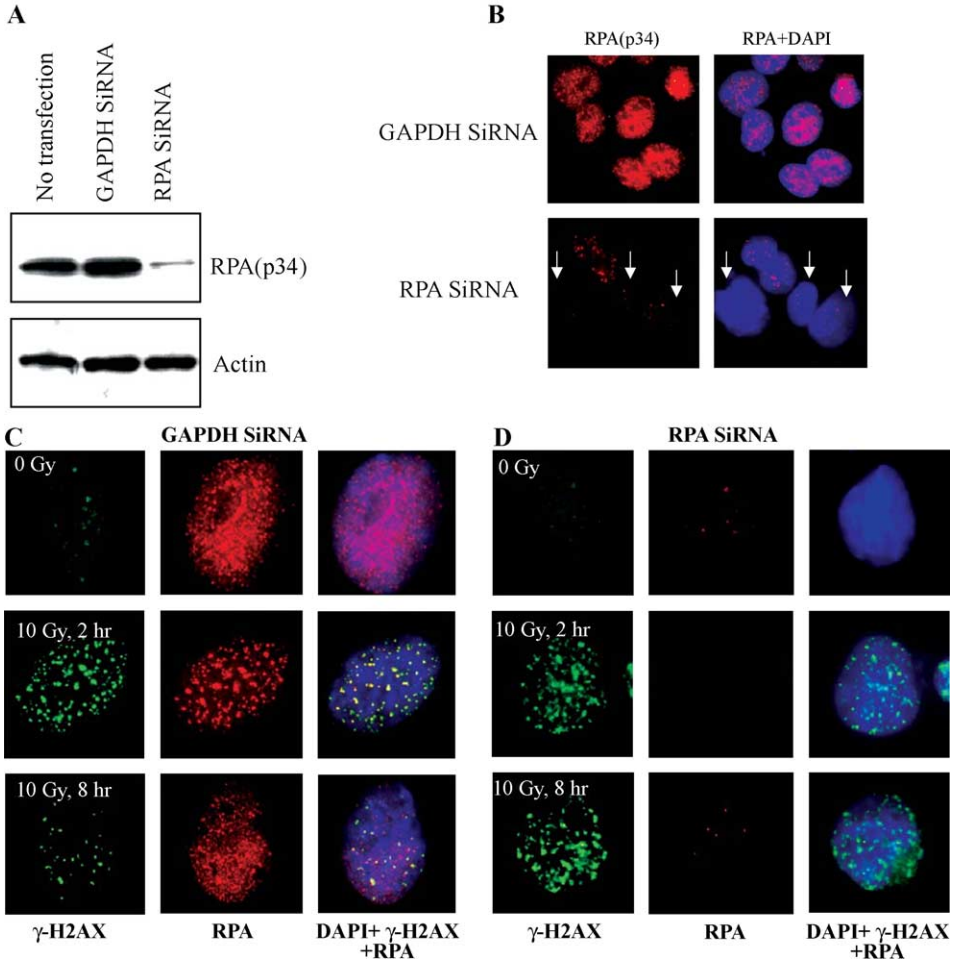

Fig. 5. RPA silencing does not affect γ-H2AX foci formation after IR. Exponentially growing GM637H cells were transfected with either control (GAPDH) or RPA SiRNA using siPORT Amine transfection reagent (Ambion). Cells were analyzed 72 h after transfection for RPA expression by Western blot (A) and immunofluorescence (B) techniques. Arrows indicate cells depleted of RPA p34 subunit by SiRNA. 50 μg of total cellular proteins isolated from control and SiRNA transfected cells was resolved on a 4–20% SDS-PAGE. RPA SiRNA-transfected cells showed a greatly reduced (90%) RPA expression as compared to nontransfected and GAPDH SiRNA-transfected cells. Immunofluorescence was carried out essentially as described before. GAPDH SiRNA (C) and RPA SiRNA (D) transfected cells were irradiated with 10 Gy of γ-rays and postincubated for 2 and 8 h. Cells were fixed in acetone–methanol (1:1) and immunostained for RPA and γ-H2AX. Nuclei were counterstained with DAPI.

γ-H2AX foci in response to IR (Figs. 5C and D). SiRNA-transfected cells were irradiated with 10 Gy of γ-rays and immunostained for both RPA and γ-H2AX. γ-H2AX foci formation in RPA-negative cells in response to IR demonstrates that γ-H2AX formation occurs independent of RPA (Fig. 5D). Unlike GAPDH SiRNA-transfected cells (Fig. 5C), γ-H2AX foci formation in RPA-depleted cells seemed to persist even at 8 h after IR more or less with the same intensity observed at 2 h (Fig. 5D).

RPA silencing enhances IR-induced micronuclei (MN) and apoptosis

Persistence of γ-H2AX in the absence of RPA may be due to unrepaired DSBs. This possibility was next examined by analyzing two commonly used biological endpoints, MN and apoptosis (both of which are due to either lack of repair or misrepair events) in IR-treated SiRNA-transfected cells (Figs. 6A and B). MN are formed during cell division when the nuclear envelope is reconstituted around chromosomes or chromosome fragments resulting from an inability to repair IR-induced DNA lesions, particularly DSBs. MN are excluded from the main nuclei, and MN frequently contain either parts of the chromosomes or whole chromosomes detected by fluorescence in situ hybridization (FISH) using DNA probes specific for centromeres, telomeres, and whole chromosomes. The formation of MN is therefore considered as a reliable marker for IR-induced chromosome breakage and loss in a wide variety of cell systems [21,22]. Induction of MN is usually analyzed in binucleated cells where the cytokinesis is effectively blocked by cytochalasin B. In blood lymphocytes, which are in G0 phase before stimulation by phytohemagglutinin (PHA), cytochalasin B is often added to score MN in cells that have divided only once after treatment. There is some debate and controversy regarding whether cytochalasin B is necessary in continuously cycling cells [21,22]. Furthermore, some studies in which MN induction has been measured after exposure to strong clastogens have indicated that, in certain cell lines with good growth characteristics and optimal culture conditions such that nuclear division occurs, the addition of cytochalasin B is not necessary [23–25]. In cycling cells, MN can be scored without cytochalasin B, but it would be difficult to differentiate between dividing and nondividing cells. Initial experiments performed in human fibroblast cells using cytochalasin B resulted in a greatly reduced number of binucleated cells after 24 h (4.2% after 10 Gy of γ-rays compared to 32% in un-irradiated cells) owing to increased cell cycle arrest at high doses of IR. Since the number of binucleated cells was extremely low, we decided to perform the experiments without cytochalasin B. Mononucleated cells without or with MN were scored per cell basis in at least 500 randomly chosen cells for each treatment, and the frequency was expressed as MN/cell. Induction of micronuclei (detected by DAPI staining) by IR was much greater in RPA SiRNA-transfected cells than nontransfected and GAPDH SiRNA-transfected cells (Table 1). Also, spontaneous level of micronuclei/cell was higher

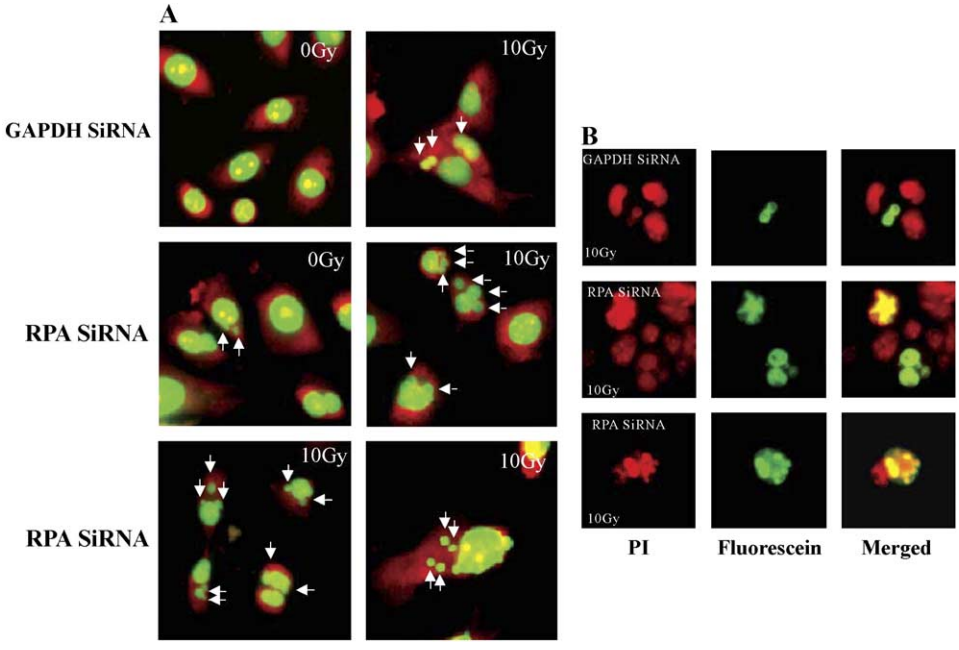

Fig. 6. RPA silencing enhances IR-induced micronuclei (MN) and apoptosis. Exponentially growing cells were treated with 10 Gy of γ-rays and incubated for 24 h. Cells were fixed in acetone–methanol for MN and 1% paraformaldehyde for TUNEL assay. MN (indicated by arrows) in mononucleated cells detected by the differential staining of cytoplasm (red) and nuclei (green) by acridine orange in SiRNA-transfected cells are shown in A. (B) Apoptotic cells induced by IR were detected by TUNEL assay (apo-BrdU-TUNEL assay, Molecular Probes) using fluorescein-conjugated antibody to BrdU. A typical apoptotic cell characterized by fragmented chromatin bodies is shown in the bottom panel. All the cells were counterstained with PI, and the apoptotic cells were easily detected by fluorescein staining.

Table 1
Analysis of micronuclei and apoptosis induction after γ-rays irradiation in GM637H cells

Treatment	Total number of cells scored	Apoptotic cells	Cells with MN	Total number of MN	MN/cell
0 Gy					
GM637H (no transfection)	1516	13 (0.8%)	73 (5.8%)	89	0.05
GM637H (GAPDH SiRNA)	842	15 (1.7%)	46 (5.4%)	37	0.05
GM637H (RPA SiRNA)	835	31 (3.7%)	57 (6.8%)	92	0.11
10 Gy					
GM637H (no transfection)	774	41 (5.3%)	139 (17.9%)	212	0.27
GM637H (GAPDH SiRNA)	699	35 (5.0%)	116 (16.5%)	221	0.31
GM637H (RPA SiRNA)	572	75 (13.1%)	136 (23.7%)	246	0.43

GM637H cells in exponential growth phase were transfected with either control SiRNA (GAPDH) or RPA SiRNA. Transfected cells in two-well chamber slides were irradiated with γ-rays (10 Gy), and the cells were fixed in acetone–methanol 24 h after treatment. The slides were immunostained for RPA and γ-H2AX followed by counterstaining with DAPI. Cells were also stained with acridine orange for MN analysis. The cells were scored for micronuclei and apoptosis. Apoptotic cells were identified by chromatin fragmentation, intense γ-H2AX staining and apo-BrdU-TUNEL assay. MN-micronuclei.

in RPA SiRNA-transfected cells probably owing to problems in DNA replication/repair in the absence of RPA (Table 1). The analysis of MN was also verified by acridine orange, which differentially stains the cytoplasm (red) and the nucleus (green). Representative figures showing MN in un-irradiated and irradiated cells transfected with GAPDH SiRNA and RPA SiRNA are given in Fig. 6A. Spontaneous and IR-induced MN were higher in RPA SiRNA-transfected cells than nontransfected and GAPDH SiRNA-transfected cells (Table 1).

We next investigated IR-induced apoptotic death in RPA depleted cells. Apoptosis determined by DNA fragmentation and intense γ-H2AX staining was greatly elevated in RPA SiRNA-transfected cells (Table 1). Apoptotic detection by DNA fragmentation was further verified by apo-BrdU-TUNEL assay kit (Molecular Probes). Both approaches yielded identical results. Representative figures demonstrating the detection of apoptotic cells by apo-BrdU-TUNEL assay are given in Fig. 6B. The apoptotic cells specifically labeled with anti-BrdU antibody conjugated with Alexa Flour 488 (fluorescein) were easily distinguished from the nonapoptotic cells. The characteristic pattern of DNA fragmentation in an apoptotic cell detected by the TUNEL assay is illustrated in the bottom panel in Fig. 6B.

Role of RPA in DNA end-joining reaction

To directly assess the role of RPA in DNA end-joining in vitro, linearized plasmid DNA substrate was used in a reaction buffer supplemented with the whole cell extracts (WCE) prepared from GM637H cells. WCE was preincubated either with or without increasing amounts of RPA antibody at 4°C for 1 h to deplete RPA from the extracts. End-joining reactions were carried out with increasing amounts of WCE to determine the optimal concentration required for end-joining (Fig. 7A). In some reactions, linearized DNA was incubated with T4 DNA ligase alone (without WCE) for comparing the pattern of ligated DNA fragments obtained with WCE in the reaction. The DNA fragments obtained with WCE in vitro exactly matched that of T4 DNA ligase indicating efficiency of the end-joining reaction. In a majority of experiments, 50 μg of WCE was used routinely, and at this concentration, 40–45% of the plasmid DNA substrate was rejoined as judged by the presence of dimers and multimers. Similar results were obtained using *Bam*HI linearized plasmid substrate. Increasing the amount of RPA antibody (0.2 to 2 μg) inhibited the

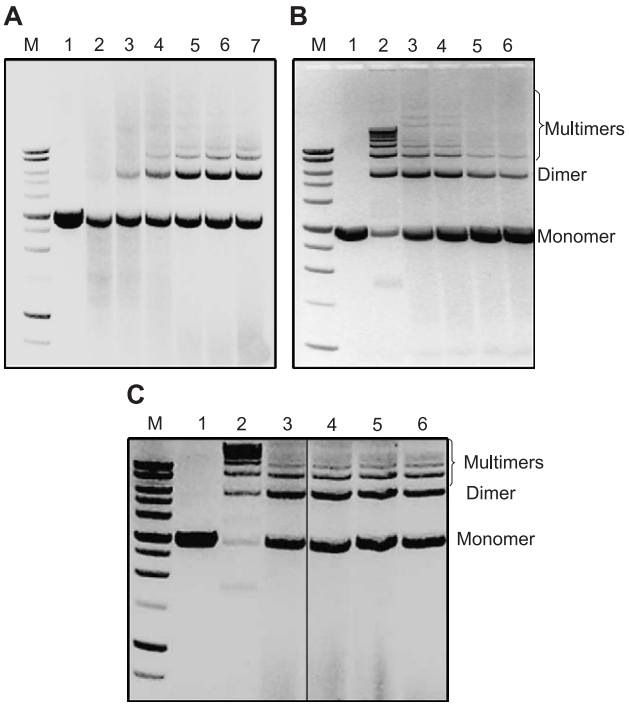

Fig. 7. RPA is required for in vitro DNA end-joining. (A) DNA end-joining reactions were carried out at 37°C for 1 h using *Eco*RI linearized Ks+ plasmid with increasing amounts of WCE prepared from GM637H cells (lanes: M–1 kb ladder marker; 1–No extract; 2 to 7–10, 20, 30, 40, 50 and 60 μg WCE). End-joining reactions either with increasing amounts of RPA (B) or γ-H2AX antibody (C) were carried out (lanes: M–1 kb ladder marker; 1–No extract; 2–T4 DNA ligase; 3–50 μg WCE; 4 to 6–0.2, 1, and 2 μg of antibody). Inverted images of ethidium bromide stained gels are given for the visual enhancement of DNA fragments.

efficiency of rejoining of dimers and multimers in a dose-dependent manner. There was a 35% reduction in the rejoining of dimers and multimers with a corresponding increase in the intensity of DNA at the monomer level at the highest concentration of RPA antibody used (Fig. 7B). In contrast to RPA, γ-H2AX antibody did not result in the inhibition of DNA end-joining (Fig. 7C). This in vitro assay clearly illustrates the effect of RPA in mediating the end-joining reaction.

Discussion

In this work, we have investigated the intranuclear dynamics of RPA foci formation and its relevance in DSB repair in human cells. To verify whether RPA foci form at the sites of DSBs, RPA foci were investigated in combination with a well-known DSB binding factor, γ-H2AX.Using two different agents to generate DSBs, we demonstrated that RPA foci colocalized with γ-H2AX in a time-dependent fashion in response to DNA strand breaks and stalled replication forks. Abolition of RPA and γ-H2AX foci formation as well as their association in cells treated with a PI-3 kinase inhibitor wortmannin indicates the involvement of different kinases in this process (data not shown). The involvement of PI-3 like kinases is partly supported by the lack of RPA and γ-H2AX colocalization in AT cells after IR. Transfection of AT cells with ATM cDNA fully restored the RPA and γ-H2AX colocalization demonstrating a regulatory role for ATM kinase in γ-H2AX and RPA assembly in response to DNA damage. Agreement between the time course of RPA and γ-H2AX foci formation and DSB repair kinetics (detected by a neutral comet assay) indicates that RPA and γ-H2AX foci association may be causally linked to DSB repair activity. Further support for a role of RPA in DSB repair is provided by the enhanced frequencies of two commonly used biological endpoints, MN and apoptosis, induced by IR in RPA silenced cells. Increased frequencies of MN and apoptosis, both of which are markers for either misrepair or lack of DSB repair, illustrate the importance of RPA in DSB repair efficiency.

The formation of phosphorylated H2AX (γ-H2AX) foci form at the sites of DSBs has been shown in a number of circumstances: (I) H2AX is phosphorylated by DNA fragmentation initiated during apoptosis [26]; (II) γ-H2AX foci form rapidly in response to DSBs in a time- and dose-dependent manner [27–30]; (III) γ-H2AX foci form at the sites of V (D) J recombination in developing thymocytes [31]; and (IV) γ-H2AX foci form at the recombinational DSBs generated during meiosis [32]. Although RPA is predominantly a relatively ubiquitous single-strand DNA-binding protein, its redistribution after DNA damage to γ-H2AX-containing focal sites indicates a probable involvement in DSB repair. In support of this contention, we have demonstrated that the depletion of RPA from cell extracts inhibits the efficiency of rejoining of plasmid DNA in vitro. Here, we find that the extent of colocalization of RPA with γ-H2AX reaches a peak at 2 h after IR. Similar observations for the colocalization of γ-H2AX with BRCA1 or Rad51 after 12 Gy of γ-rays have been made by Paull et al. [33] who showed that γ-H2AX facilitates DSB repair by recruiting factors such as BRCA1, Rad50, and Rad51 proteins that are involved in the homologous recombination repair pathway. The recruitment of BRCA1 to γ-H2AX sites preceded that of Rad50 and Rad51 proteins, and DNA repair-defective cell lines have a reduced capacity to phosphorylate H2AX. A functional interaction of RPA with Rad51 and Rad52 proteins has been documented in earlier studies [34,35]. Hence, the colocalization of γ-H2AX with RPA described here together with the report of similar association between γ-H2AX and BRCA1 or Rad51 in foci [33] suggests that RPA may also be a cog in the recombination repair machinery for DSBs.

RPA plays dynamic roles in diverse DNA excision repair pathways, and a role in DSB repair has recently emerged. The formation and persistence of RPA foci formation have been demonstrated in human lymphoblastoid cells after IR, but the functional significance of this foci formation largely remains obscure [17]. In this study, we have shown that the focal distribution of RPA triggered by IR coincides with γ-H2AX sites in a time-dependent manner. Although RPA and γ-H2AX foci association was detectable at 30 min, the extent of colocalization peaked at 2 h consistent with the 'slow' component of DSB repair ($t_{1/2}$ estimated between 1 and 4 h) reported in the literature [36–38]. It has been suggested that in DSB repair-deficient cells, the 'slow' repair component is more vulnerable to error-prone repair leading to more unstable and stable chromosomal alterations. RPA and γ-H2AX assembly in foci may be to optimize the efficiency of 'slow' component of DSB repair activity. This notion is supported by the high incidence of spontaneous and induced chromosomal instability in H2AX null cells [39,40].

An accessory role for RPA in DSB rejoining in vitro by a nonhomologous end-joining (NHEJ) pathway has been recently demonstrated [15]. In corroboration, we have provided evidence for a role for RPA in DNA end-joining in this study. Recently, Kobayashi et al. [41] using a cell-free assay detected RPA foci in response to DSBs in *Xenopus* nuclei. An analogous situation in human cells is presented in this study by the colocalization of RPA with a well-known DSB binding factor γ-H2AX in response to both IR and HU. A few recent reports also demonstrated RPA and γ-H2AX foci formation upon replication blockage imposed by adozelesin, methyl methanesulfonate and HU [42–44]. Similar to the findings of this study, Liu et al. [42,43] demonstrated the induction of RPA and γ-H2AX foci formation as well as RPA hyperphosphorylation in S-phase cells after treatment with HU and adozelesin. RPA hyperphosphorylation induced by adozelesin, but not HU, was abolished by pretreatment of cells with a DNA polymerase inhibitor aphidicolin, which blocks the replication fork progression. This observation suggests that

active replication forks are required for adozelesin-induced DNA damage but not for HU which may directly act on replication fork machinery [43]. Furthermore, HU-induced γ-H2AX foci formation was attenuated in ATR kinase-defective cells, while RPA foci remained essentially the same indicating the requirement of ATR kinase for HU-induced γ-H2AX foci formation [43]. Nevertheless, lack of complete abolition of γ-H2AX foci formation after HU in ATR kinase-defective cells indicates that kinases other than ATR may also be involved in this process. The same may be true for RPA foci formation induced by HU, which was unaffected in ATR kinase-defective cells [43]. Although we have not evaluated the role of either ATR or ATM in HU-induced RPA and γ-H2AX foci formation, we have convincingly demonstrated that ATM kinase is required for both RPA and γ-H2AX foci formation and colocalization in response to IR-induced DSBs. This is in support of earlier studies [28,29], which showed the requirement of ATM and ATR kinases for IR and replication stress-induced H2AX phosphorylation, respectively. Although Liu et al. [43] demonstrated the focalization of RPA and γ-H2AX individually after HU treatment, it was not clear whether these two proteins colocalized at the same sites. This study provides a clear evidence for the assembly of both proteins in response to HU-induced DSBs. On the basis of our findings, we suggest that DSBs generated at the stalled replication forks trigger the phosphorylation of RPA and H2AX leading to their recruitment to the lesion sites. Once bound, RPA and γ-H2AX complex may impose an efficient S-phase checkpoint control by recruiting additional DNA repair and replication proteins to the sites of lesions. Together, all these studies mentioned above suggest the possibility that RPA and γ-H2AX foci assembly may constitute one of the S-phase checkpoint responses, which is solely dependent on stalled replication forks. A recent study indicates a preferential association of hyperphosphorylated RPA with sites of DNA damage containing γ-H2AX, ATR, and Rad51 [44]. These authors have suggested that the preferential association of repair factors with the modified form of RPA would provide a mechanism to recruit the essential DSB repair factors to the sites of DNA damage. Our observation of DNA damage-dependent assembly of RPA and γ-H2AX after IR and HU provides credence to this suggestion.

It is likely that RPA binds to DNA strand breaks generated by IR, thereby preventing degradation of genomic DNA by exonuclease digestion. Alternatively, RPA together with γ-H2AX may preserve the strand alignment and suppress the illegitimate recombination at the DNA break sites. This possibility is strongly supported by the recruitment of both RPA and γ-H2AX to the stalled replication forks generated by HU. The functional assembly of RPA with γ-H2AX as well as PCNA at the DNA breaks generated by replication blockage indicates that RPA-associated protein complexes may constitute an important component of DNA replication checkpoint control machinery. Shao et al. [9] reported hyperphosphorylation of RPA by DNA-PK in response to camptothecin treatment resulting in the dissociation of RPA-DNA-PK complex. They proposed that the blockage of a replication fork at a topoisomerase–DNA cleavable complex could lead to a juxtaposition of replication fork-associated RPA and DNA double-strand associated DNA-PK, leading to RPA hyperphosphorylation which in turn may constitute the signal for S-phase checkpoint machinery. It is not clear whether a similar mechanism also operates for IR- and HU-induced S-phase arrest. Nevertheless, it is interesting to note that ATM cells, which are deficient in RPA phosphorylation, lack S-phase checkpoint control after IR treatment.

It is likely that the chromatin modification induced by DSBs may be the primary trigger for H2AX phosphorylation, which may help in opening the chromatin, thereby facilitating DSB repair by recruiting other repair factors. Abolition of H2AX phosphorylation by a PI-3 kinase inhibitor also affects the assembly of other repair factors such as BRCA1, Rad50, and Rad51 proteins [33]. Cells from H2AX null mice, which are deficient in recruitment of DSB repair factors after IR [39,40], showed increased chromosomal instability probably due to misrepaired DNA strand breaks. This illustrates that H2AX and its phosphorylation may be a vital component in the recognition and repair of DSBs. In support, we observed that the abolition of H2AX phosphorylation by wortmannin also affects RPA foci formation after IR (data not shown). It is likely that the phosphorylation status of histone H2AX is critical for the recruitment of RPA to DSB sites. The gradual coincidence of RPA with γ-H2AX containing focal sites in a time-dependent fashion might indicate a key role for RPA in protecting the ends of the DNA and enhancing the DSB repair process. Absence of RPA and γ-H2AX foci assembly in AT cells after IR strongly suggests that ATM plays a key role in the organization of this complex. A role for ATM kinase in both RPA and H2AX phosphorylation has been demonstrated [10,28]. Additionally, colocalization of ATM foci with γ-H2AX at DSB sites has been documented [45]. Although inhibition of histone H2AX phosphorylation by wortmannin affects RPA foci formation, it is not clear whether RPA phosphorylation per se is a prerequisite for its recruitment to γ-H2AX containing sites. In cells treated with HU, we found specific enrichment of phosphorylated RPA in the chromatin-bound protein fraction, which also contained γ-H2AX. Use of phosphorylation-specific RPA antibodies is required to determine which form of RPA binds to γ-H2AX containing DSB sites induced by IR.

RPA together with γ-H2AX at DNA break sites may stabilize and protect the broken DNA ends from degradation during the repair processes and enhance the rejoining of DNA strand breaks by preserving strand alignment. Additionally, γ-H2AX and RPA coassembly may constitute the damage recognition step for an efficient repair of DSB rejoining. In support, we have shown that depletion of RPA

by SiRNA enhanced the DNA damaging effects of IR in terms of micronuclei and apoptosis induction. Overall, the single-strand DNA-binding protein RPA appears to be a significant player in a wide range of DNA damage recognition, cell cycle control and repair pathways with profound influence on the maintenance of genomic stability.

Acknowledgments

This work was supported by research grants awarded to C.R.G. from DHHS, NIH (CA 75061, CA 49062 and RR-11623), DOE Office of Science (BER) (DEFG0298ER62687).

References

[1] C. Iftode, Y. Daniely, J.A. Borowiec, Replication protein A (RPA): the eukaryotic SSB, Crit. Rev. Biochem. Mol. Biol. 34 (1999) 141–180.
[2] Z. He, L.A. Henricksen, M.S. Wold, C.J. Ingles, RPA involvement in the damage-recognition and incision steps of nucleotide excision repair, Nature 374 (1995) 566–569.
[3] B.E. Lee, J.W. Sung, D.K. Kim, D.K.J.R. Lee, N.D. Kim, S.W. Kang, Functional studies on the interaction between human replication protein A and xeroderma pigmentosum group A complementing protein (XPA), Mol. Cells 9 (1999) 185–190.
[4] T. Matsuda, M. Saijo, I. Kuraoka, T. Kobayashi, Y. Nakatsu, A. Nagai, T. Enjoji, C. Masutani, K. Sugasawa, F. Hanaoka, A. Yasui, K. Tanaka, DNA repair protein XPA binds replication protein A (RPA), J. Biol. Chem. 270 (1995) 4152–4157.
[5] T. Matsunaga, C.H. Park, T. Bessho, D. Mu, A. Sancar, Replication protein A confers structure-specific endonuclease activities to the XPF-ERCC1 and XPG subunits of human DNA repair excision nuclease, J. Biol. Chem. 271 (1996) 11047–11050.
[6] G.L. Dianov, B.R. Jensen, M.K. Kenny, V.A. Bohr, Replication protein A stimulates proliferating cell nuclear antigen-dependent repair of abasic sites in DNA by human cell extracts, Biochemistry 38 (1999) 11021–11025.
[7] T.A. Ranalli, M.S. DeMott, R.A. Bambara, Mechanism underlying replication protein A stimulation of DNA ligase I, J. Biol. Chem. 277 (2002) 1719–1727.
[8] M.S. Park, D.L. Ludwig, E. Stigger, S.H. Lee, Physical interaction between human RAD52 and RPA is required for homologous recombination in mammalian cells., J. Biol. Chem. 271 (1996) 8996–19000.
[9] R.G. Shao, C.X. Cao, H. Zhang, K.W. Kohn, M.S. Wold, Y. Pommier, Replication mediated DNA damage by camptothecin induces phosphorylation of RPA by DNA-dependent protein kinase and dissociates RPA: DNA-PK complexes, EMBO J. 18 (1999) 1397–1406.
[10] H. Wang, J. Guan, A.R. Perrault, Y. Wang, G. Iliakis, Replication protein A2 phosphorylation after DNA damage by the coordinated action of ataxia telangiectasia-mutated and DNA-dependent protein kinase, Cancer. Res. 61 (2001) 8554–8563.
[11] D.K. Kim, E. Stigger, S.H. Lee, Role of the 70-kDa subunit of human replication protein A (I). Single-stranded DNA binding activity, but not polymerase stimulatory activity, is required for DNA replication, J. Biol. Chem. 271 (1996) 15124–15129.
[12] M. Gatei, S.P. Scott, I. Filippovitch, N. Soronika, M.F. Lavin, B. Weber, K.K. Khanna, Role for ATM in DNA damage-induced phosphorylation of BRCA1, Cancer Res. 60 (2000) 3299–3304.
[13] M. Gatei, D. Young, K.M. Cerosaletti, A. Desai-Mehta, K. Spring, S. Kozlov, M.F. Lavin, R.A. Gatti, P. Concannon, K.K. Khanna, ATM-dependent phosphorylation of nibrin in response to radiation exposure, Nat. Genet. 25 (2000) 115–119.
[14] A.W. Plug, A.H. Peters, Y. Xu, K.S. Keegan, M.F. Hoekstra, D. Baltimore, P. de Boer, T. Ashley, ATM and RPA in meiotic chromosome synapsis and recombination, Nat. Genet. 17 (1997) 457–461.
[15] R. Perrault, N. Cheong, H. Wang, G. Iliakis, RPA facilitates rejoining of DNA double-strand breaks in an in vitro assay utilizing genomic DNA as substrate, Int. J. Radiat. Biol. 77 (2001) 593–607.
[16] S.K. Choudhary, R. Li, BRCA1 modulates ionizing radiation-induced nuclear focus formation by the replication protein A p34 subunit, J. Cell. Biochem. 84 (2002) 666–674.
[17] S.H. MacPhail, P.L. Olive, RPA foci are associated with cell death after irradiation, Radiat. Res. 155 (2001) 672–679.
[18] Y. Ziv, A. Bar-Shira, I. Pecker, P. Russell, T.J. Jorgensen, I. Tsarfati, Y. Shiloh, Recombinant ATM protein complements the cellular AT-phenotype, Oncogene 15 (1997) 159–167.
[19] M. Wojewodzka, I. Buraczewska, M. Kruszewski, A modified neutral comet assay: elimination of lysis at high temperature and validation of the assay with anti-single-stranded DNA antibody, Mutat. Res. 518 (2002) 9–20.
[20] A.S. Balajee, C.R. Geard, Chromatin-bound PCNA complex formation triggered by DNA damage occurs independent of the ATM gene product in human cells, Nucleic Acids Res. 29 (2001) 1341–1351.
[21] M. Aardema, M. Kirsch-Volders, The in vivo micronucleus assay, in: Wai Nag Choy (Ed.), Genetic Toxicology and Cancer Risk Assessment, Marcel Dekker, New York, 2001, pp. 163–186.
[22] M. Kirsch-Volders, T. Sofuni, M. Aardema, S. Albertini, D. Eastmond, M. Fenech, M. Ishidate Jr., E. Lorge, H. Norppa, J. Surralles, H.W. von der, A. Wakata, Report from the in vitro micronucleus assay working group, Environ. Mol. Mutagen. 35 (2000) 167–172.
[23] H. Stopper, M. Full, R. Helbig, G. Speit, Micronucleus induction by neocarzinostatin and methyl methanesulfonate in ionizing radiation-sensitive Chinese hamster V79 cell mutants, Mutat. Res. 383 (1997) 107–112.
[24] S. Kalweit, D. Utesch, H.W. von der, S. Madle, Chemically-induced micronucleus formation in V 79 cells—Comparison of three different test approaches, Mutat. Res. 439 (1999) 183–190.
[25] T. Matsushima, M. Hayashi, A. Matsuoka, M. Ishidate Jr., K.F. Miura, H. Shimizu, Y. Suzuki, K. Morimoto, H. Ogura, K. Mure, K. Koshi, T. Sofuni, Validation study of the in vitro micronucleus test in a Chinese hamster lung cell line (CHL/IU), Mutagenesis 14 (1999) 569–580.
[26] E.P. Rogakou, W. Nieves-Neira, C. Boon, Y. Pommier, W.M. Bonner, Initiation of DNA fragmentation during apoptosis induces phosphorylation of H2AX histone at serine 139, J. Biol. Chem. 275 (2000) 9390–9395.
[27] E.P. Rogakou, D.R. Pilch, A.H. Orr, V.S. Ivanova, W.M. Bonner, DNA double-stranded breaks induce histone H2AX phosphorylation on serine 139, J. Biol. Chem. 273 (1998) 5858–5868.
[28] S. Burma, B.P. Chen, M. Murphy, A. Kurimasa, D.J. Chen, ATM phosphorylates histone H2AX in response to DNA double-strand breaks, J. Biol. Chem. 276 (2001) 42462–42467.
[29] I.M. Ward, J. Chen, Histone H2AX is phosphorylated in an ATR-dependent manner in response to replicational stress, J. Biol. Chem. 276 (2001) 47759–47762.
[30] E.P. Rogakou, C. Boon, C. Redon, W.M. Bonner, Megabase chromatin domains involved in DNA double-strand breaks in vivo, J. Cell Biol. 146 (1999) 905–916.
[31] H.T. Chen, A. Bhandoola, M.J. Difilippantonio, J. Zhu, M.J. Brown, X. Tai, E.P. Rogakou, T.M. Brotz, W.M. Bonner, T. Ried, A. Nussenzweig, Response to RAG-mediated VDJ cleavage by NBS1 and gamma-H2AX, Science 290 (2000) 1962–1965.
[32] S.K. Mahadevaiah, J.M. Turner, F. Baudat, E.P. Rogakou, P. de Boer, J. Blanco-Rodriguez, M. Jasin, S. Keeney, W.M. Bonner, P.S. Burgoyne, Recombinational DNA double strand breaks in mice precede synapsis, Nat. Genet. 27 (2001) 271–276.

[33] T.T. Paull, E.P. Rogakou, V. Yamazaki, C.U. Kirchgessner, M. Gellert, W.M. Bonner, A critical role for histone H2AX in recruitment of repair factors to nuclear foci after DNA damage, Curr. Biol. 10 (2000) 886–895.
[34] E.I. Golub, R.C. Gupta, T. Haaf, M.S. Wold, C.M. Radding, Interaction of human rad51 recombination protein with single-stranded DNA binding protein, RPA, Nucleic Acids Res. 26 (1998) 5388–5393.
[35] S.L. Gasior, A.K. Wong, Y. Kora, A. Shinohara, D.K. Bishop, Rad52 associates with RPA and functions with Rad55 and Rad57 to assemble meiotic recombination complexes, Genes Dev. 12 (1998) 2208–2221.
[36] B. Stenerlow, E. Hoglund, J. Carlsson, E. Blomquist, Rejoining of DNA fragments produced by radiations of different linear energy transfer, Int. J. Radiat. Biol. 76 (2000) 549–557.
[37] H. Hoglund, B. Stenerlow, Induction and rejoining of DNA double-strand breaks in normal human skin fibroblasts after exposure to radiation of different linear energy transfer: possible roles of track structure and chromatin organization, Radiat. Res. 155 (2001) 818–825.
[38] B. Stenerlow, E. Hoglund, Rejoining of double-stranded DNA-fragments studied in different size-intervals, Int. J. Radiat. Biol. 78 (2002) 1–7.
[39] C.H. Bassing, K.F. Chua, J. Sekiguchi, H. Suh, S.R. Whitlow, J.C. Fleming, B.C. Monroe, C.D.N. Ciccone, C. Yan, K. Vlasakova, D.M. Livingston, D.O. Ferguson, R. Scully, F.W. Alt, Increased ionizing radiation sensitivity and genomic instability in the absence of histone H2AX, Proc. Natl. Acad. Sci. U. S. A. 99 (2002) 8173–8178.
[40] A. Celeste, S. Petersen, P.J. Romanienko, O. Fernandez-Capetillo, H.T. Chen, O.A. Sedelnikova, B. Reina-San-Martin, V. Coppola, E. Meffre, M.J. Difilippantonio, C. Redon, D.R. Pilch, A. Olaru, M. Eckhaus, R.D. Camerini-Otero, L. Tessarollo, F. Livak, K. Manova, W.M. Bonner, M.C. Nussenzweig, A. Nussenzweig, Genomic instability in mice lacking histone H2AX, Science 296 (2002) 922–927.
[41] T. Kobayashi, S. Tada, T. Tsuyama, H. Murofushi, M. Seki, T. Enomoto, Focus-formation of replication protein A, activation of checkpoint system and DNA repair synthesis induced by DNA double-strand breaks in *Xenopus* egg extract, J. Cell Sci. 115 (2002) 3159–3169.
[42] J.S. Liu, S.R. Kuo, T.A. Beerman, T. Melendy, Induction of DNA damage response by adozelesin is S phase-specific and dependent on active replication forks, Mol. Cancer Ther. 2 (2003) 41–47.
[43] J.S. Liu, S.R. Kuo, T. Melendy, Comparison of checkpoint response triggered by DNA polymerase inhibition versus DNA damaging agents, Mutat. Res. 532 (2003) 215–226.
[44] V.M. Vassin, M.S. Wold, J.A. Borowiec, Replication protein A (RPA) phosphorylation prevents RPA association with replication centers, Mol. Cell. Biol. 24 (2004) 1930–1943.
[45] Y. Andegeko, L. Moyal, L. Mittelman, I. Tsarfaty, Y. Shiloh, G. Rotman, Nuclear retention of ATM at sites of DNA double strand breaks, J. Biol. Chem. 276 (2001) 38224–38230.